Interference between second-harmonic generation from a substrate and from an adsorbate layer

G. Berkovic* and Y. R. Shen

Department of Physics, University of California, Berkeley, Berkeley, California 94720

G. Marowsky and R. Steinhoff

Max-Planck-Institut für Biophysikalische Chemie, Abteilung Laserphysik, Postfach 2841, D-3400 Göttingen, Federal Republic of Germany

Received November 3, 1987; accepted October 27, 1988

Several experiments on surface second-harmonic generation are presented to show how the contribution from a transparent substrate can interfere with that from an adsorbate monolayer. The interference depends on the relative phase of the two contributions, which varies with the molecular orientation, the laser frequency, the polarization, and the optical geometry.

INTRODUCTION

In recent years optical second-harmonic generation (SHG) has developed into a useful probe of adsorbate molecules on surfaces.[1,2] It has been applied to a wide variety of adsorbate-covered surfaces, ranging from single crystals under ultrahigh vacuum conditions[3,4] to liquids and amorphous solids under ambient conditions.[5–11] From these experiments it is possible to deduce concentration and orientation of molecular adsorbates[5] as well as to observe desorption,[4] two-dimensional phase transitions,[6] and chemical reactions[7] of the adsorbed species. Furthermore, SHG from a monolayer of an adsorbate molecular species has been used for measuring second-order nonlinear-optical coefficients of molecules.[8,9]

The fact that SHG can be used as a surface probe for such a wide variety of uses stems from the high surface selectivity and specificity inherent in SHG. This is because, as a second-order process, SHG is forbidden under the electric-dipole approximation in a medium with central symmetry, but the symmetry is necessarily broken at a surface.[12] Consider, for example, SHG from reflection at an air–solid interface. The effective surface nonlinear polarization responsible for the SHG is given by[13]

$$\mathbf{P}_s^{(2)}(2\omega) = \vec{\chi}_s^{(2)}:\mathbf{E}(\omega)\mathbf{E}(\omega). \tag{1}$$

Here the effective surface nonlinear susceptibility $\chi_s^{(2)}$ actually consists of two terms: one from the symmetry-broken surface layer and the other from the bulk of the solid. If the bulk has an inversion symmetry, then its contribution to $\chi_s^{(2)}$ can come only from the electric-quadrupole and magnetic-dipole parts and thus becomes comparable with, or less than, the surface contribution. In many cases it is even much smaller than the surface contribution.

With a monolayer of adsorbates on the surface, the surface nonlinear susceptibility can be written as

$$\chi_s^{(2)} = \chi_{\text{sub}}^{(2)} + \chi_{\text{ads}}^{(2)}, \tag{2}$$

where $\chi_{\text{sub}}^{(2)}$ denotes the effective surface nonlinear susceptibility of the bare substrate in the absence of the adsorbates and $\chi_{\text{ads}}^{(2)}$ refers to the change of the surface susceptibility resulting from the adsorption of the monolayer. Note that here $\chi_{\text{ads}}^{(2)}$ includes the contribution arising from the adsorbate–substrate interaction. In general, all $\chi^{(2)}$'s are complex quantities. Molecular adsorption can increase or decrease the total susceptibility $\chi_s^{(2)}$.

For metals and semiconductors the adsorbates can drastically modify the surface states and surface optical transitions.[14] The change in $\chi_s^{(2)}$ is usually difficult to analyze, particularly if ω and 2ω are close to resonant transitions. The case of molecular adsorbates on transparent insulators is often much simpler. Here, if the substrate adsorption lies well above both ω and 2ω, $\chi_{\text{sub}}^{(2)}$ can be taken as real. If the absorption bands of the adsorbates are also well above ω and 2ω, then $\chi_{\text{ads}}^{(2)}$ is also real. The relative sign between $\chi_{\text{sub}}^{(2)}$ and $\chi_{\text{ads}}^{(2)}$ depends on the orientation of the adsorbate molecules on the substrate.

When ω or 2ω is scanned through an adsorbate resonance, $\chi_{\text{ads}}^{(2)}$ becomes complex, and thus $\chi_s^{(2)}$ should also vary accordingly. In a normal experiment only the quantities $|\chi_s^{(2)}|$ and $|\chi_{\text{sub}}^{(2)}|$ are determined. To find $\chi_{\text{ads}}^{(2)}$ the relative phase factors of $\chi_s^{(2)}$ and $\chi_{\text{sub}}^{(2)}$ must be known. They can be obtained by an interference method developed by Chang *et al.*,[15] by Tom *et al.*,[16] and by Kemnitz *et al.*[17] The phase measurements are particularly important in cases when $\chi_{\text{ads}}^{(2)} \approx \chi_{\text{sub}}^{(2)}$, even if we care to know only $\chi_{\text{ads}}^{(2)}$. For $\chi_{\text{ads}}^{(2)} \gg \chi_{\text{sub}}^{(2)}$, we have the approximation $\chi_s^{(2)} = \chi_{\text{ads}}^{(2)}$, which was used to find $\chi_{\text{ads}}^{(2)}$ in several recent experiments.[8–11]

In this paper we demonstrate, by using a number of examples, the importance of phases associated with the surface nonlinear susceptibilities for adsorbates on transparent substrates. Destructive interference between $\chi_{\text{sub}}^{(2)}$ and $\chi_{\text{ads}}^{(2)}$ can be observed for polar molecules of sufficiently low surface densities adsorbed onto a substrate. We have verified that $\chi_{\text{ads}}^{(2)}$ changes from real to complex as the laser frequency

0740-3224/89/020205-04$02.00

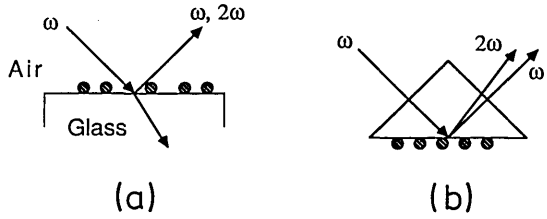

Fig. 1. SHG from an adsorbate-covered substrate in (a) simple reflection and (b) TIR geometries at air–glass interfaces. Wave-vector conservation causes the fundamental and second-harmonic beams to emerge collinearly in the simple reflection geometry but not in the TIR geometry.

scans a two-photon resonance. It is observed that a given substrate–adsorbate system may exhibit destructive interference in one SHG geometry but not in another because of the different Fresnel factors and dominant $\chi_s^{(2)}$ components associated with the different geometries. All these examples suggest that, in deducing $\chi_{ads}^{(2)}$ from the SHG measurements and in using it to study molecular adsorbates, we must be careful to subtract the substrate contribution from the measured results properly.

EXPERIMENTAL

Substrates used in this study were either glass or fused-silica slides and prisms that had been precleaned in an oxidizing acid solution (e.g., sulfuric acid/hydrogen peroxide). The molecules used as adsorbates were 4′-(*n*-octyl)-4-cyanobiphenyl (8CB), 4-dimethylaminopyridine (DAP), and Rhodamine 110. Adsorption of different adsorbate surface densities was achieved by dipping a substrate into isopropyl alcohol solutions of these molecules at various concentrations.

The setup for SHG experiments has been described elsewhere.[9,18] Two types of measurement were performed. In one type SHG signals were measured directly by photon counting of the second-harmonic intensity in the light reflected from the sample. In the second type of experiment (for measurements of relative phases),[19] a crystalline quartz plate on a translation stage is inserted into the setup immediately after reflection from the sample. In this case we measure the interference in the SHG signals generated by the sample and the quartz as the separation between them is varied. This interference results from the different dispersions of the refractive indices at ω and 2ω in air and appears as a periodic pattern with a period

$$L_c = \lambda/[2(n_{2\omega} - n_\omega)], \tag{3}$$

where λ is the fundamental wavelength and n_ω is the refractive index in air at the frequency ω. The relative phase factor of the surface susceptibility is deduced from a comparison of this interference pattern with one generated by using the same translatable quartz plate and either a reference (e.g., the bare substrate) or a standard (e.g., a quartz crystal of known chirality).[17]

Two different geometries were used for SHG experiments. One geometry was the simple reflection geometry [Fig. 1(a)] and the other was the total internal reflection (TIR) geometry [Fig. 1(b)]. Because the fundamental and the second-harmonic beams do not emerge from the prism collinearly in the TIR geometry, phase measurements were not attempted in that geometry. In all measurements the fundamental was a tunable dye laser, providing pulses of approximately 5-mJ energy, 10-nsec duration, and 10-Hz repetition rate.

RESULTS AND DISCUSSION

Figure 2(a) shows how the second-harmonic signal varies as the 8CB coverage on glass is increased. In this case the simple reflection geometry [Fig. 1(a)] was used. The fundamental input at 750 nm was *s* polarized, and the second-harmonic output was *p* polarized, so the surface susceptibility component measured is $[\chi_s^{(2)}]_{zyy}$. The samples were prepared by dipping the glass substrates into progressively more concentrated solutions of 8CB for a sufficiently long time to achieve equilibrium for surface adsorption. The surface coverage of 8CB is expected to be linearly proportional to the concentration of 8CB in the solution because we limited our measurements to the low-concentration limit.

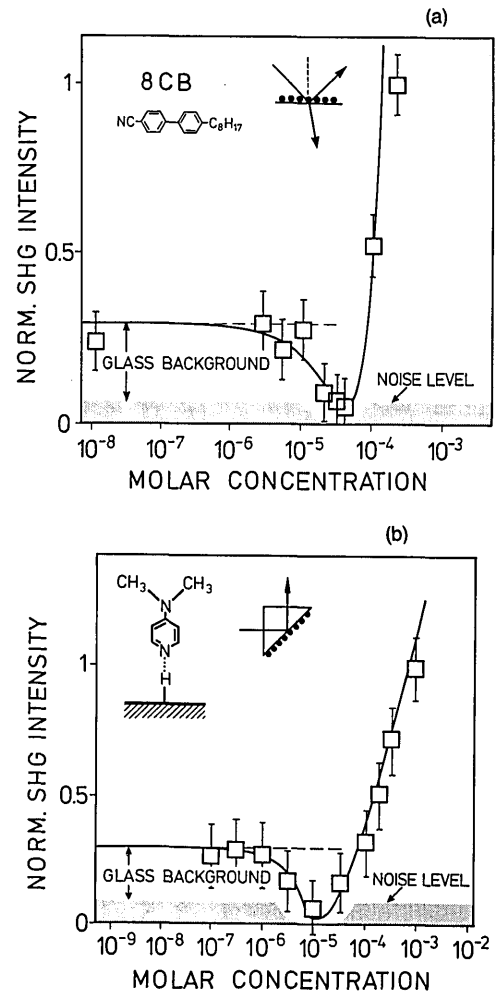

Fig. 2. SHG intensities from two selected adsorbate-covered substrates as a function of concentration of adsorbate dipping solution used. The curves are least-squares fits to Eq. (4). (a) 8CB on glass, in simple reflection, with *s*-polarized 750-nm fundamental and *p*-polarized SHG output. (b) DAP on fused silica, in TIR geometry, with *s*-polarized 720-nm fundamental and *p*-polarized SHG output.

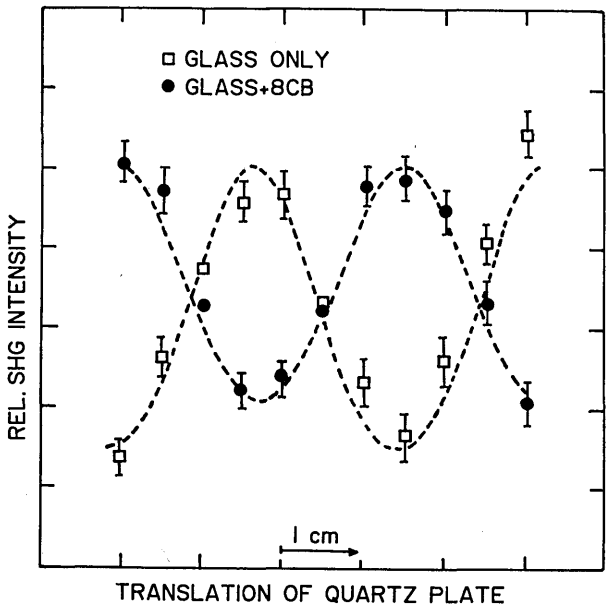

Fig. 3. Comparison of interferences obtained when a second harmonic is generated from both the sample (glass and 8CB-coated glass) and a crystalline quartz plate mounted onto a translation stage. The fundamental (700 nm) was *s* polarized, and the second harmonic was *p* polarized in simple reflection. The dashed curves are fits to the theoretical interference band shape $y = [A + B \sin(2\pi x/L_c)]^2$, where $L_c = 3.6 \pm 0.1$ cm, as given by Eq. (3).

As shown in Fig. 2(a), the data can be fitted by the simple expression

$$\text{SH signal} \propto |\chi_s^{(2)}|^2 = |\chi_{\text{sub}}^{(2)} - N\beta|^2, \tag{4}$$

where N is the molar concentration of 8CB in the solution and both $\chi_{\text{sub}}^{(2)}$ and β are positive real quantities. The results indicate that $\chi_{\text{ads}}^{(2)}$ for 8CB on glass is real and negative, with $\chi_{\text{sub}}^{(2)}$ of glass taken to be positive. This is understandable because both ω and 2ω are well below the absorption bands of 8CB, and it is known that the 8CB molecules adsorb on glass with their polar heads pointing toward the glass. [Note that our assignment taking $\chi_{\text{sub}}^{(2)}$ of glass as positive is arbitrary; we have not performed an absolute calibration, as described by Kemnitz *et al.*[17]]

We would expect that DAP molecules adsorbed onto fused silica should yield similar results with ω and 2ω in the transparent region because they also have their polar heads pointing toward the substrate. This is indeed the case. We show in Fig. 2(b) the results obtained with the TIR geometry [Fig. 1(b)] by using *s*-polarized input and *p*-polarized output. Again the data are well described by Eq. (4).

To verify further that $\chi_{\text{sub}}^{(2)}$ and $\chi_{\text{ads}}^{(2)}$ are opposite in sign (180° out of phase), we can measure the phases of $\chi_s^{(2)}$ with and without adsorbate explicitly by using the interference method mentioned above. Figure 3 shows the interference patterns of the second-harmonic signal generated in simple reflection from both the plain glass and the 8CB-covered glass as a function of the position of the crystalline quartz plate. The 8CB coverage here was chosen so as to yield a second-harmonic signal that was approximately equal to that of the plain glass. It is seen that the two patterns in Fig. 3 are exactly 180° out of phase. This confirms the result that $[\chi_{\text{sub}}^{(2)}]_{zyy}$ of glass and $[\chi_{\text{ads}}^{(2)}]_{zyy}$ for 8CB on glass have opposite signs. We also note that the two interference patterns conform to the expected $(A + B \sin 2\pi x/L_c)^2$ shape with the correct value of the periodicity, $L_c = 3.6$ cm, as predicted by Eq. (3).

To examine the change in phase of $\chi_{\text{ads}}^{(2)}$ as the input laser frequency is increased such that 2ω falls within the adsorbate absorption band, we have determined the phase of $\chi_{\text{ads}}^{(2)}$ for Rhodamine 110 on glass at several wavelengths. Measurements were performed in simple reflection by using *p*-polarized fundamental input and *p*-polarized harmonic output. The Rhodamine 110 surface coverage was chosen so as to yield approximately four times the second-harmonic signal of plain glass. At all wavelengths interference patterns were measured for both the plain glass and the Rhodamine-covered slide. In all cases satisfactory interference patterns, displaying the correct periodicity as predicted by Eq. (3), were obtained. From the interference patterns, the relative phase of $\chi_s^{(2)}$ is obtained, which, together with the ratio of magnitudes $|\chi_{\text{sub}}^{(2)}|:|\chi_s^{(2)}|$, yields the relative phase of $\chi_{\text{ads}}^{(2)}$, as shown by Fig. 4.

The relative phase, $\Delta\phi_{\text{ads}}$, of $\chi_{\text{ads}}^{(2)}$ for Rhodamine 110 on glass at various wavelengths is given in Fig. 5. Off resonance ($\lambda = 742$ nm), $\Delta\phi_{\text{ads}} = 0$, increasing as expected to $\Delta\phi_{\text{ads}} \approx \pi/2$ for $\lambda = 662$ nm, when 2ω coincides with the peak of an absorption band.

Our studies of Rhodamine 110 on glass revealed a surpris-

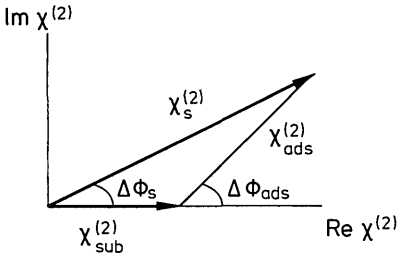

Fig. 4. Vectorial relations between $\chi_{\text{ads}}^{(2)}$, $\chi_s^{(2)}$, $\chi_{\text{sub}}^{(2)}$ and relative phases.

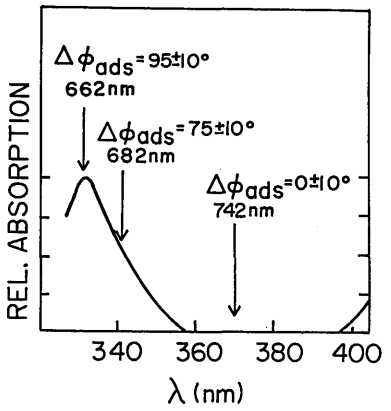

Fig. 5. The relative phase, $\Delta\phi_{\text{ads}}$, for Rhodamine 110 on glass is shown at various wavelengths. The effect of the second-harmonic frequency's entering into resonance with the S_0–S_2 absorption is shown by comparison with the absorption spectrum (measured in isopropyl alcohol solution) of Rhodamine 110. The absorption beginning at ≈400 nm is the edge of the S_0–S_1 transition.

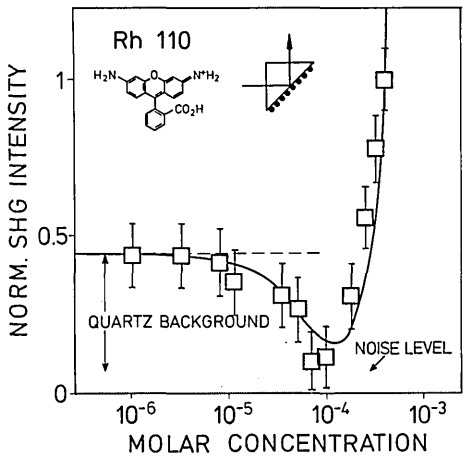

Fig. 6. SHG intensity from Rhodamine 110-covered silica substrate in TIR geometry with p-polarized fundamental input at 720 nm and p-polarized SHG output. The curve is the best fit to expression (4).

ing phenomenon. When we used the same polarization combinations (both fundamental and harmonic p polarized), different intensity-versus-coverage behavior was observed in simple reflection and TIR geometries. As shown above, in the simple reflection geometry, $\Delta\phi_{ads} = 0$ at 742 nm, and consequently the total SHG signal was observed to increase monotonically with increasing Rhodamine coverage. However, in TIR geometry (see Fig. 6) SHG cancellation behavior was observed to be similar to that for 8CB and DAP, as shown in Figs. 2(a) and 2(b). These results suggest that $\chi^{(2)}_{sub}$ and $\chi^{(2)}_{ads}$ are of the same sign in simple reflection but have opposite signs in TIR. Note that the p-input–p-output polarizations used probe a linear combination of three χ components given by

$$[F_1\chi^{(2)}_{xzx} + F_2\chi^{(2)}_{zzz} + F_3\chi^{(2)}_{zxx}]_{sub} + [F_1\chi^{(2)}_{xzx} + F_2\chi^{(2)}_{zzz} + F_3\chi^{(2)}_{zxx}]_{ads}. \quad (5)$$

Here F_i are products of appropriate Fresnel factors, depending on the geometry.[12,20,21] These Fresnel factors differ greatly (signs, relative magnitudes) from simple reflection to TIR. Appropriate values of the various $\chi^{(2)}_s$ components of $\chi^{(2)}_{sub}$ and $\chi^{(2)}_{ads}$ substituted into Eq. (5) could explain the different second-harmonic signal-versus-coverage behavior observed in the two geometries; however, the experimental data reported here are insufficient to permit extraction of the values of the individual χ^2_s components that are necessary to verify this. Further experiments aimed at elucidating this point are in progress.

In summary, using several examples, we have demonstrated how a transparent substrate may contribute to the surface SHG and may interfere with the second-harmonic signal from the adsorbate. Phase measurements are obviously necessary for the separation of the two contributions. This is particularly important when the two contributions are comparable in magnitude.

ACKNOWLEDGMENTS

We thank Xudong Xiao for assistance with some of the measurements. G. Berkovic acknowledges support from the Yeda Fund. Research at the University of California, Berkeley, was supported by the Minnesota Mining and Manufacturing Company through the Office of Energy Research, Office of Basic Energy Sciences, Materials Sciences Division of the U.S. Department of Energy, under contract DE-AC03-76SF00098.

G. Berkovic and Y. R. Shen are also affiliated with the Center for Advanced Materials, Lawrence Berkeley Laboratory, Berkeley, California 94720.

* Present address, Department of Structural Chemistry, Weizmann Institute of Science, Rehovot, 76100 Israel.

REFERENCES

1. Y. R. Shen, Ann. Rev. Mater. Sci. **16,** 69 (1986); in *New Laser and Optical Investigations of Chemistry and Structure of Interfaces*, R. B. Hall and A. B. Ellis, eds. (Verlag Chemie, Weinheim, 1986), p. 151.
2. G. L. Richmond, H. M. Rojhantalab, J. M. Robinson, and V. L. Shannon, J. Opt. Soc. Am. B **4,** 228 (1987).
3. J. M. Chen, J. R. Bower, C. S. Wang, and C. H. Lee, Opt. Commun. **9,** 132 (1973).
4. X. D. Zhu, Y. R. Shen, and R. Carr, Surf. Sci. **163,** 114 (1985).
5. T. F. Heinz, H. W. K. Tom, and Y. R. Shen, Phys. Rev. A **28,** 1883 (1983).
6. Th. Rasing, Y. R. Shen, M. W. Kim, and S. Grubb, Phys. Rev. Lett. **55,** 2903 (1985).
7. G. Berkovic, Th. Rasing, and Y. R. Shen, J. Chem. Phys. **85,** 7374 (1986).
8. I. R. Girling, N. A. Cade, P. V. Kolinsky, J. D. Earls, G. H. Cross, and I. R. Peterson, Thin Solid Films **132,** 101 (1985).
9. G. Berkovic, Th. Rasing, and Y. R. Shen, J. Opt. Soc. Am. B **4,** 945 (1987).
10. O. A. Aktsipetrov, N. N. Akhmediev, I. M. Baranova, E. D. Mishina, and V. R. Novak, Sov. Phys. JETP **62,** 524 (1985).
11. G. Marowsky, A. Gierulski, and B. Dick, Opt. Commun. **52,** 339 (1985).
12. Y. R. Shen, *The Principles of Nonlinear Optics* (Wiley, New York, 1984), Chap. 25.
13. P. Guyot-Sionnest, W. Chen, and Y. R. Shen, Phys. Rev. B **33,** 8254 (1986); P. Guyot-Sionnest and Y. R. Shen, Phys. Rev. B **35,** 4420 (1987).
14. H. W. K. Tom, C. M. Mate, X. D. Zhu, J. E. Crowell, Y. R. Shen, and G. A. Somorjai, Surf. Sci. **172,** 466 (1986); H. W. K. Tom, X. D. Zhu, Y. R. Shen, and G. A. Somorjai, Surf. Sci. **167,** 167 (1986).
15. R. K. Chang, J. Ducuing, and N. Bloembergen, Phys. Rev. Lett. **15,** 6 (1965).
16. H. W. K. Tom, T. F. Heinz, and Y. R. Shen, Phys. Rev. Lett. **51,** 1983 (1983).
17. K. Kemnitz, K. Bhattacharyya, J. M. Hicks, G. R. Pinto, K. B. Eisenthal, and T. F. Heinz, Chem. Phys. Lett. **131,** 285 (1986).
18. Th. Rasing, G. Berkovic, Y. R. Shen, S. G. Grubb, and M. W. Kim, Chem. Phys. Lett. **130,** 1 (1986).
19. H. W. K. Tom, Ph.D. dissertation (University of California, Berkeley, Berkeley, Calif., 1985).
20. P. Guyot-Sionnest, H. Hsuing, and Y. R. Shen, Phys. Rev. Lett. **57,** 2963 (1986).
21. T. F. Heinz, Ph.D. dissertation (University of California, Berkeley, Berkeley, Calif., 1983).